

On the Compensation of Delay in the Discrete Frequency Domain

Gareth Parker

*Defence Science and Technology Organisation, P.O. Box 1500, Edinburgh, South Australia 5111, Australia
Email: gareth.parker@dsto.defence.gov.au*

Received 31 October 2003; Revised 19 February 2004; Recommended for Publication by Ulrich Heute

The ability of a DFT filterbank frequency domain filter to effect time domain delay is examined. This is achieved by comparing the quality of equalisation using a DFT filterbank frequency domain filter with that possible using an FIR implementation. The actual performance of each filter architecture depends on the particular signal and transmission channel, so an exact general analysis is not practical. However, as a benchmark, we derive expressions for the performance for the particular case of an allpass channel response with a delay that is a linear function of frequency. It is shown that a DFT filterbank frequency domain filter requires considerably more degrees of freedom than an FIR filter to effect such a pure delay function. However, it is asserted that for the more general problem that additionally involves frequency response magnitude modifications, the frequency domain filter and FIR filters require a more similar number of degrees of freedom. This assertion is supported by simulation results for a physical example channel.

Keywords and phrases: frequency domain, FDAF, transmultiplexer, equaliser, delay.

1. INTRODUCTION

The term “frequency domain adaptive filter” (FDAF) [1] is often applied to any adaptive digital filter that incorporates a degree of frequency domain processing. Some time domain adaptive filtering algorithms, such as the least mean square (LMS), may be well approximated using such “frequency domain” processing, by employing fast Fourier transform (FFT) algorithms to perform the necessary convolutions [1]. The computational complexity of such implementations of these adaptive filters can be, for a large number of taps, considerably less than the explicit time domain forms. It is this computational advantage that is often the main motivation for using these architectures. Other advantages also exist, such as the ability to achieve a uniform rate for all convergence modes (see, e.g., [1]).

Architectures that could be more deservedly labelled “frequency domain” can be achieved by transforming the time domain input signal into a form in which individual frequency components can be directly modified. This process can be approximated using a filterbank “analyser” [2], shown in Figure 1, which channels the input $x(n)$ into relatively narrow, partially overlapping subbands, or “bins.” For clarity of illustration, the complex oscillator inputs to the multipliers in the analyser, $e^{-j2\pi n f_k / f_s}$, are denoted simply by $-f_k$, $k = 0 \dots K - 1$. In the synthesiser, the conjugate oscillators $e^{j2\pi n f_k / f_s}$ are similarly denoted by f_k .

With a sampling frequency f_s Hz, the output of a K bin filterbank analyser with decimation M at time mM/f_s is a vector of bins $\mathbf{X}(m) = [X(m, f_0), \dots, X(m, f_{K-1})]$. The k th bin contains an estimate of the complex envelope of the narrow bandpass filtered component of $x(n)$ centred at f_k Hz. If the bins are uniformly spaced between $-f_s/2$ and $f_s/2$, then the filterbank can be implemented using the discrete Fourier transform (DFT) and it is then known as a DFT filterbank [2]. As with other frequency domain filters, computationally efficient implementations of the DFT filterbank, incorporating FFT algorithms, also exist [2]. When used for frequency domain filtering, the DFT filterbank is sometimes also known as a transmultiplexer [1, 3].

The contents of the bins can be modified by multiplication with possibly time varying, complex scalar weights $\mathbf{W}(m) = [W(m, f_0), \dots, W(m, f_{K-1})]$, so that filtering is performed in a manner that is analogous to the explicit application of a transfer function to the Fourier transform of a continuous time signal. A filterbank synthesiser reconstitutes a time domain output $y(n)$ by appropriately combining the modified bins $\mathbf{Y}(m) = [Y(m, f_0), \dots, Y(m, f_{K-1})]$.

Importantly, it is possible to design the filterbank so that the contents of a particular frequency bin can be modified, with relatively little impact on adjacent frequency components. This approximate independence can be achieved by designing the analysis and synthesis lowpass filters, $h(n)$

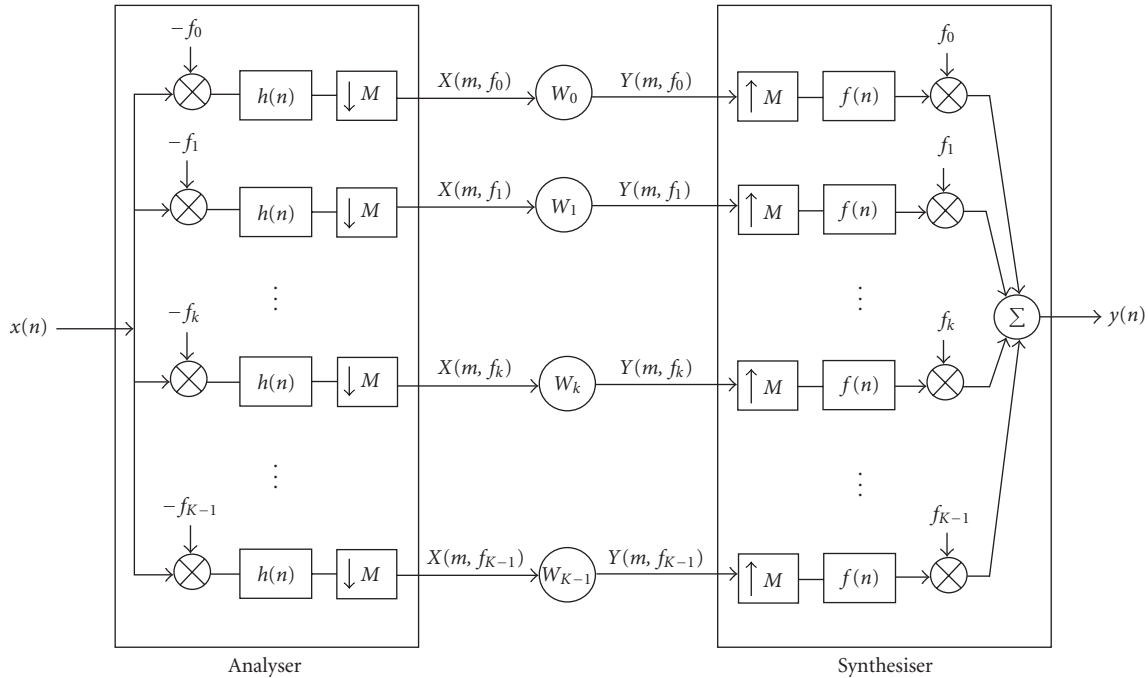


FIGURE 1: K -channel DFT filterbank conceptual diagram.

and $f(n)$, respectively, so that only adjacent bins experience significant spectral overlap. This can be achieved, to almost arbitrary precision, by using appropriately long impulse responses, N_h and N_f for $h(n)$ and $f(n)$. In FDAF applications, it is typical [1] to design $N_h = N_f = RK$, where R is around 3 or 4. Approximate bin independence is ideal for filtering functions whose main objective is the modification of spectral magnitude, such as “interference excision” (see, e.g., [4, 5]), a narrowband interference mitigation technique in which frequency components that comprise strong interference have weights set equal to zero. In that application, the smaller the overlap between adjacent filterbank bins, the better. However, this is not necessarily the case in applications that require a delay to be applied to the signal. The ability to effect delay is important in applications such as channel equalisation, echo cancellation, and the exploitation of cyclostationarity [6]. The requirement may vary from the need to effect a constant delay, as in a noise canceller, through to the equaliser requirement that the delay may be frequency dependent.

Figure 2 shows an example to illustrate the limitations of the DFT filterbank FDAF. A source signal $s(n)$ is transmitted over a channel and is received as $x(n)$. A delayed version of $s(n)$ is available as a desired response signal, $d(n) = s(n - \lambda)$. A filter is to be designed to process $x(n)$ to make it as “close” as possible to $d(n)$. Assume that the channel is such that $x(n)$ is equal to $s(n)$, other than for a delay that may vary with frequency, but that is constant within each bin width of an FDAF solution. A time domain adaptive filter solution may be to filter $x(n)$ using a finite impulse response (FIR) filter,

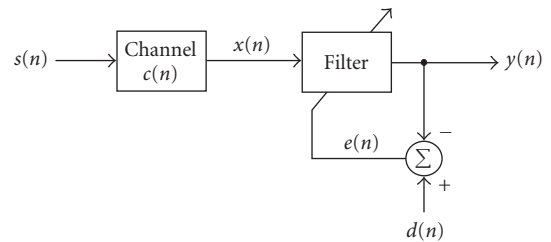


FIGURE 2: Example filtering problem.

with a tap weight vector $\mathbf{w}(n)$ that is adapted according to the error $e(n) = d(n) - y(n)$ using an algorithm such as LMS [7].

With an FDAF solution, both $x(n)$ and $d(n)$ are channelised into approximate frequency domain representations $X(m, f_k)$ and $D(m, f_k)$. Each frequency component, $X(m, f_k)$, is multiplied by a complex scalar $W(m, f_k)$ so that $Y(m, f_k) = W(m, f_k)X(m, f_k)$, and the inverse transform is then applied to generate $y(n)$, the estimate of $d(n)$. Figure 3 shows an illustration of this filtering process.

If bin independence is assumed, the objective can be achieved by making, for every bin, $Y(m, f_k)$ as close as possible to $D(m, f_k)$ and the frequency domain weights vector can also be optimised using simple algorithms such as LMS [1]. Let the delay that the transmission channel has imposed on the k th filterbank bin of the primary signal be denoted by ℓ . If the filterbank decimates the time domain data by a factor of M , then the delays λ and ℓ become λ/M and ℓ/M samples,

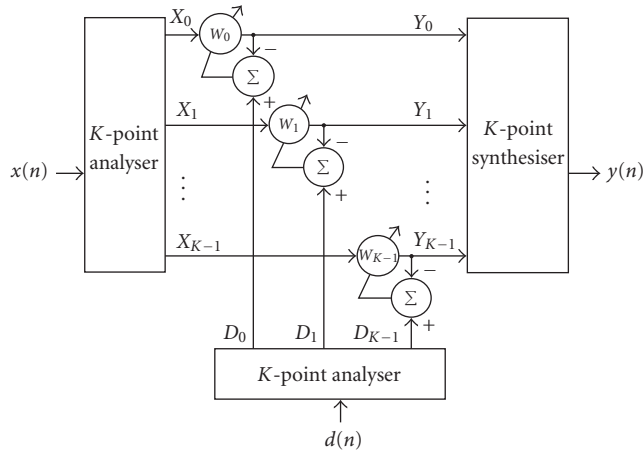


FIGURE 3: K -channel frequency domain adaptive filter.

respectively, and we require

$$\begin{aligned} W(m, f_k) S\left(m - \frac{\ell}{M}, f_k\right) \\ \approx D(m, f_k) = S\left(m - \frac{\lambda}{M}, f_k\right) \\ \Rightarrow W(m, f_k) S(m, f_k) \approx S\left(m - \frac{(\lambda - \ell)}{M}, f_k\right). \end{aligned} \quad (1)$$

Equality is clearly not possible. In general, modification of the magnitude and phase within a filterbank bin is not sufficient to perfectly achieve *any* nontrivial delay. In this paper, we present an analysis to quantitatively determine the degree to which a filterbank FDAF can compensate or effect delay. The paper is structured as follows. A discussion of previous related research is given in the next section. In Section 3, an analysis is presented of the accuracy with which an FIR filter can compensate a delay that varies linearly over a specified bandwidth. This is useful both for the explicit purpose of analysis of the FIR filter and also for the analysis in Section 4 of the FDAF, which can be viewed as comprising a single tap FIR filter operating within each filterbank bin. Section 4 includes a comparison between FIR and FDAF delay compensation for linear delay channels, as well as a simulation example for a real-world channel. Conclusions are summarised in Section 5.

2. PREVIOUS ANALYSES OF THE FREQUENCY DOMAIN DELAY COMPENSATION PROBLEM

In 1981, Reed and Feintuch [8] compared the performance of an adaptive noise canceller, implemented using the time domain LMS algorithm, with an early “frequency domain” LMS approximation. The particular frequency domain architecture that was studied was that of Dentino et al. [9], which approximated the LMS algorithm using a combination of FFT/IFFT algorithms that resulted in circular convolutions. A particular observation in [8] is that if the time and frequency domain filters are implemented using the same

number of degrees of freedom¹ and if there exists differential delay between the primary and desired response inputs, then excessive noise appears in the frequency domain solution. Although the amount of excess noise is quantified, the results in [8] are applicable only to that particular “frequency domain” filter.

Sometimes, particularly for the equaliser and echo canceller problems, a subband adaptive filter (SAF) is adopted [10, 11, 12, 13, 14, 15]. A SAF is a generalisation of a FDAF, where a multitap FIR adaptive filter operates within each filterbank channel. The ability of the SAF to effect a performance that is comparable to a time domain implementation has been recently addressed in [10, 12, 16]. In [12], the use of critically sampled filterbanks for the system identification problem has been examined. For the identification of a system with an impulse response comprising L_s samples, it is stated that the number of FIR taps within each subband filter should be around

$$L = \frac{L_s + N_h + N_f}{M}, \quad (2)$$

where the filterbank analysis and synthesis filters have lengths N_h and N_f , respectively, and the filterbank decimates the sampling rate by a factor M . In [16], the result of [12] is applied to the equaliser problem, and it is argued that to achieve the same performance as an L_{td} tap time domain equaliser, the number of samples in each FIR filter must be around

$$L = \frac{L_{td} + N_h}{M}. \quad (3)$$

In [10], a similar expression is provided, although the factor N_h in the numerator of (3) is doubled. This is essentially the same as (2), except that the application is different. The correctness of the expression for the equalisation problem is justified in [10] through simulation results, but it is acknowledged as a conservative relationship. Although it is appropriate for the case where $L \gg 1$, where L is close to one or, in the case of the FDAF, equal to one, the expression is less suitable. Equation (3) suggests that there is no filterbank FDAF which can achieve the performance of a FIR filter. For instance, if $N_h = RK = RMI$, where I is the oversampling factor, then even as $K \rightarrow \infty$, $L \rightarrow RI$. There is a need to determine guidelines for the choice of K in a filterbank FDAF, where $L = 1$, and this is the focus of this paper.

3. EFFECTING DELAY USING AN FIR FILTER

In order to determine the degree to which a DFT filterbank FDAF can effect delay, we will determine the estimation error that is associated with each filterbank bin and then combine these errors in a frequency domain SNR measure. In some applications, this may be the most appropriate measure of quality. In others, including conventional equalisers and

¹That is, the number of bins in the frequency domain implementation is equal to the number of time domain taps.

noise cancellers, it may be more appropriate to measure the SNR associated with the filterbank output. These two SNR measures will be identical for an “ideal” filterbank; that is, one that exhibits perfect reconstruction and which has independent bins. If the bins are not independent but exhibit some spectral overlap, then the relationship between the frequency and time domain SNR measures is only approximate. In the following discussion, we will analyse the error within the filterbank bins by treating each bin as an optimal single tap, linear time invariant (LTI) FIR filter. Consequently, we first obtain a general expression for the performance of an optimal FIR equaliser. This will also be useful for the purpose of comparison between the FIR and the filterbank. Further comparison with an SAF is detailed in [6].

Consider an L -tap FIR filter, with f_s Hz sampling rate. A delay can be exactly effected if it is equal to an integer multiple, less than L , of $1/f_s$ second. For delays not equal to a multiple of $1/f_s$, the delay will be an approximation [17], the accuracy of which can be determined by considering the optimum FIR filter.

To analyse this, we will elaborate on the example shown in Figure 2. Consider the transmission of a zero-mean signal $s(t)$ through a channel with impulse response $c(t)$. At a receiver, this is sampled and applied to an L -tap FIR filter as the observation signal, $x(n) = s(n) * c(n)$, where $s(n)$ and $x(n)$ are the sampled signals and $c(n)$ is the equivalent discrete-time channel. The filter produces the output $y(n) = \mathbf{w}\mathbf{x}_n$, where $\mathbf{x}_n = [x(n-L+1), \dots, x(n)]^T$ contains the last L signal samples and the FIR filter impulse response is contained within the row vector $\mathbf{w} = [w(0), \dots, w(L-1)]$. A desired response, $d(n)$, is provided, which is related to $s(n)$ by $d(n) = s(n) * g(n)$, where $g(n)$ is assumed to have an FIR. Ideally, $s(n)$ would be available at the receiver and $g(n)$ would then be a simple delay, designed into the adaptive filter and chosen so that the equalisation problem has a causal solution. Assume that $s(n)$ is stationary and define the autocorrelation matrix and cross-correlation vector as

$$\mathbf{R} = \begin{pmatrix} R_{xx}(0) & \cdots & R_{xx}(-L+1) \\ \vdots & R_{xx}(0) & \vdots \\ R_{xx}(L-1) & \cdots & R_{xx}(0) \end{pmatrix}, \quad (4)$$

$$\mathbf{p} = [R_{dx}(0), \dots, R_{dx}(L-1)],$$

where $R_{xx}(\tau) = E[x(n)x^*(n-\tau)]$ and $R_{dx}(\tau) = E[d(n)x^*(n-\tau)]$. The weights vector that minimises the mean square estimation error (MSE) is the Wiener solution, $\mathbf{w} = \mathbf{p}\mathbf{R}^{-1}$. Standard analysis (see, e.g., [7]) shows that the error power is equal to

$$J = E\{|d(n) - y(n)|^2\} \\ = R_{dd}(0) - \mathbf{p}\mathbf{R}^{-1}\mathbf{p}^H \quad (5)$$

and so the SNR at the filter output can be expressed as

$$\text{SNR} = \frac{R_{dd}(0)}{R_{dd}(0) - \mathbf{p}\mathbf{R}^{-1}\mathbf{p}^H}. \quad (6)$$

This can be further manipulated in terms of the source signal power $\sigma^2 = E[s(n)s^*(n)]$ and the impulse responses of the channels $c(n)$ and $g(n)$. Assuming that $s(n)$ is stationary, it can be shown [6] that

$$R_{dd}(\tau) = R_{ss}(\tau) * R_{gg}(\tau), \\ R_{dx}(\tau) = R_{ss}(\tau) * R_{gc}(\tau), \quad (7) \\ R_{xx}(\tau) = R_{ss}(\tau) * R_{cc}(\tau),$$

where we have defined $R_{gc}(\tau) = g(\tau) * c^*(-\tau)$, $R_{gg}(\tau) = g(\tau) * g^*(-\tau)$, and $R_{cc}(\tau) = c(\tau) * c^*(-\tau)$.

Now let $s(n)$ be a white stationary signal and consider the ideal equalisation problem where $g(n)$ is a delay of λ samples, chosen to facilitate a causal solution. Thus $g(n) = \delta(n-\lambda)$ so that $d(n) = s(n-\lambda)$ and $R_{dd}(0) = R_{ss}(0) = \sigma^2$. Then, from equation (5), the MSE is equal to

$$J = \sigma^2 - \frac{1}{\sigma^2} \sum_{i=0}^{L-1} |R_{dx}(i)|^2. \quad (8)$$

As $s(n)$ is white with variance σ^2 , then $R_{dx}(\tau) = \sigma^2\delta(\tau-\lambda) * c^*(-\tau) = \sigma^2c^*(-\tau+\lambda)$. Thus, in this case, we have

$$J = \sigma^2 \left(1 - \sum_{i=0}^{L-1} |c^*(\lambda-i)|^2 \right) \quad (9)$$

and the SNR is equal to

$$\text{SNR} = \frac{1}{1 - \sum_{i=0}^{L-1} |c^*(\lambda-i)|^2}. \quad (10)$$

Let the channel $c(n)$ have a bandpass frequency response with a delay that varies linearly from ℓ_{\min} to ℓ_{\max} samples, over a filter bandwidth of $2b$ bins, in an N -sample DFT of the impulse response $c(n)$. It can be shown [6] that the discrete magnitude frequency response can be written as

$$C(k) = \text{rect}\left(\frac{k}{2b}\right) e^{j\Phi(k)}, \quad (11)$$

where the phase response is given by

$$\Phi(k) = (\ell_{\min} - \ell_{\max}) \frac{\pi k^2}{2bN} - (\ell_{\max} + \ell_{\min}) \frac{\pi k}{N}. \quad (12)$$

Example 1 (constant delay channel). A particularly simple special case of the linear delay channel is when the delay is constant, equal to ℓ samples, where ℓ is *not* necessarily an integer. In this case, if the channel bandwidth extends over the sampling frequency range, then $f_c = f_s/2$ and $c(n) = \text{sinc}(n-\ell)$. Then, from equation (10),

$$\text{SNR} = \frac{1}{1 - \sum_{i=0}^{L-1} |\text{sinc}(\lambda-\ell-i)|^2}. \quad (13)$$

Clearly, if $\lambda - \ell$ is a multiple of the sampling period but is less than L , then the sinc function is sampled only at its peak and at its zero crossings. In this case, the summation in the denominator of (13) equals unity and the SNR is infinite.

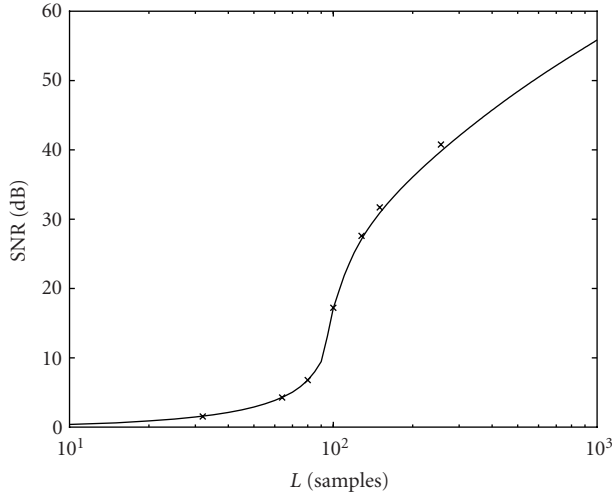


FIGURE 4: Reconstruction SNR for FIR equalisation of linear delay channel.

This verifies the earlier statement that an FIR filter is capable of perfectly achieving delays which are a multiple of the tap spacing. However, recall that ℓ is not necessarily an integer. If a noninteger delay is required, then the sinc function will not be sampled at its zero crossings and the SNR is finite. A perfect noninteger delay cannot be achieved for finite L .

Example 2 (general linear delay channel). Next we look at the equalisation of a channel with a delay which varies linearly over a 100-sample range. In this case, we examine both theoretical and experimental performances. In order to assure a causal experimental channel with a delay response which closely approximates the desired response, we let the number of samples in the channel impulse response be $N_{ch} = 2048$ and design the delay to vary from sample 975 to sample 1075, symmetric about $n_0 = 1025$. Figure 4 shows the theoretical SNR for an optimal L point FIR equaliser for this channel. The curve was generated using (12) and (11) to numerically evaluate (10). Also shown by crosses are the experimental results. The parameter λ was chosen to maximise the summation of equation (10). As $|c(n)|$ is symmetric about sample n_0 , this means choosing $\lambda = (L - 1)/2 + n_0$ and, in this example, we have $\lambda = (L - 1)/2 + 1025$ samples. Experimental results, obtained for a unity variance complex Gaussian white noise signal and using an LMS algorithm to approximate the optimal filter, are indicated by crosses.

4. FILTERBANK

The analysis of Section 3 can be used to determine the accuracy with which a filterbank FDF can compensate delay by considering the FIR case with $L = 1$ taps. However, by allowing an arbitrary number of FIR taps, the study can be generalised to a SAF [6]. A subband adaptive equaliser can be implemented using identical filterbanks to generate each of the primary $X(m, f_k)$ and desired $D(m, f_k)$ response signals

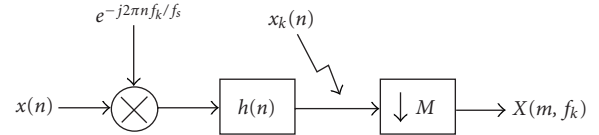


FIGURE 5: Signal flow diagram for the k th channel of the filterbank analyser, processing the observation signal $x(n)$.

from the time domain inputs $x(n)$ and $d(n)$. An FIR filter is independently applied to each channel of $X(m, f_k)$ to minimise the performance criterion, which is assumed here to be the MSE. The error power associated with each bin is readily determined using the analysis of Section 3 for the FIR filter. If the filterbanks are capable of perfect reconstruction with independent bins, then the sum of the error power within each bin of this equaliser equals the MSE of the time domain estimate of $d(n)$. An expression for the equaliser SNR can be readily determined. If the filterbank does not satisfy these properties, then such an expression is only approximate.

To facilitate the application of the general FIR filter analysis of Section 3, let the signal $s(n)$ pass through the transmission channels $c'(n)$ and $g'(n)$ to produce the observation and desired response signals $x(n) = s(n) * c'(n)$ and $d(n) = s(n) * g'(n)$. The signal within the k th observation filterbank bin is, prior to decimation,

$$x_k(n) = [(s(n) * c'(n))e^{-j2\pi f_k n / f_s}] * h(n), \quad (14)$$

as illustrated in Figure 5. Similarly,

$$d_k(n) = [(s(n) * g'(n))e^{-j2\pi f_k n / f_s}] * h(n). \quad (15)$$

These can be shown to be equivalent to

$$\begin{aligned} x_k(n) &= (s(n)e^{-j2\pi f_k n / f_s}) * (c'(n)e^{-j2\pi f_k n / f_s}) * h(n), \\ d_k(n) &= (s(n)e^{-j2\pi f_k n / f_s}) * (g'(n)e^{-j2\pi f_k n / f_s}) * h(n). \end{aligned} \quad (16)$$

Let $s_k(n) = s(n)e^{-j2\pi f_k n / f_s}$, $c'_k(n) = c'(n)e^{-j2\pi f_k n / f_s}$, and $g'_k(n) = g'(n)e^{-j2\pi f_k n / f_s}$ so that we can write

$$\begin{aligned} x_k(n) &= s_k(n) * c'_k(n) * h(n), \\ d_k(n) &= s_k(n) * g'_k(n) * h(n). \end{aligned} \quad (17)$$

Writing $c_k(n) = c'_k(n) * h(n)$ and $g_k(n) = g'_k(n) * h(n)$ gives us expressions for $x(n)$ and $d(n)$ in the form of the general FIR analysis. That is,

$$\begin{aligned} x_k(n) &= s_k(n) * c_k(n), \\ d_k(n) &= s_k(n) * g_k(n). \end{aligned} \quad (18)$$

This means that expressions for $R_{x_k x_k}(n)$, $R_{d_k d_k}(n)$, and $R_{d_k x_k}(n)$, and thus the SNR within each channel, can be easily determined. After decimation by M , the observation and desired response signals are $X(m, f_k) = x_k(mM)$ and $D(m, f_k) = d_k(mM)$, respectively. Assuming no aliasing occurs, the correlation functions of the decimated data are $R_{X_k X_k}(m) = R_{x_k x_k}(mM)$, $R_{D_k D_k}(m) = R_{d_k d_k}(mM)$, and

$R_{D_k X_k}(m) = R_{d_k X_k}(mM)$. Further analysis requires particular cases to be treated separately. We assume throughout that $s(n)$ has unity variance and is white over the frequency range $-f_s/2$ to $f_s/2$.

4.1. Frequency domain filter

A filterbank FDAF has $L = 1$ and expression (6) for the SNR within the k th bin reduces to

$$\text{SNR}_k = \frac{R_{D_k D_k}(0)}{R_{D_k D_k}(0) - |R_{D_k X_k}(0)|^2 / R_{X_k X_k}(0)}. \quad (19)$$

We now proceed to determine the correlation functions for a channel that has flat magnitude response with linear delay. This is achieved by inverse Fourier transforming the corresponding cross-spectra. The magnitude of the cross-spectrum between the desired response and observation signals within a particular bin is bandpass from approximately $-f_s/2K$ to $f_s/2K$ Hz. Under the assumption that the transmission channels $c'(n)$ and $g'(n)$ are flat with unity gain over the bandwidth of each bin, the shape of the cross-spectrum is determined solely by the frequency response of the analysis filters and $\mathcal{S}_{ss}(f)$, the power spectral density of $s(n)$. That is, $\mathcal{S}_{d_k X_k}(f) = |H(f)|^2 \mathcal{S}_{ss}(f - f_k)$, as shown in the appendix. Since we assume that $s(n)$ is white over the frequency range between $-f_s$ and f_s Hz, then $\mathcal{S}_{ss}(f) = \sigma^2/f_s$. The cross-spectral phase is bin dependent but is simply the difference between the phase response of the channels over this frequency range. This can be determined from the corresponding delay difference. Thus the cross-correlation function for each bin, $R_{D_k X_k}(m)$, can be determined using an algorithm for designing a linear delay FIR filter.

Although we derive results for a filterbank with a practical analysis filter, it is also essential to consider the ideal, independent bin case. The reason for this is threefold; first, the assumption of independent bins is frequently made in frequency domain filtering applications; second, we will see that this extreme filterbank architecture achieves the worst possible delay performance; and third, simple closed-form expressions can be obtained for its performance. If the filterbank satisfies the perfect reconstruction property and has independent bins, then the analysis filter has an ideal brick-wall frequency response that is flat between $-f_s/2K$ and $f_s/2K$ Hz. That is, $H(f) = \text{rect}(f/2f_c)$, where $f_c = f_s/2K$ Hz.

4.1.1. Equalisation of a constant delay channel using an ideal filterbank

It is useful to explicitly consider the case where the channel delay is constant since, as will now be shown, a closed-form expression for the SNR can be derived. Let the transmission channel $c'(n)$ have a constant delay equal to ℓ samples, where ℓ is not necessarily an integer, and let $g'(n)$ have a constant λ sample delay. The delay difference between $g'(n)$ and $c'(n)$ is thus $\lambda - \ell$. The bandwidth of each bin is equal to $2f_c = f_s/K$ and so the magnitude of $\mathcal{S}_{d_k X_k}(f)$ is equal to $\mathcal{S}_{ss}(f) \text{rect}(fK/f_s)$. At the decimated sample rate, $f'_s = f_s/M$, the cross-spectral bandwidth becomes $2f'_c = f_s M/K$ and the ‘‘filter’’ group delay is $(\lambda - \ell)/M$. The impulse response $p(m)$,

whose discrete-time Fourier transform equals the cross-spectrum $\mathcal{S}_{d_k X_k}(f)$, can be shown to equal

$$p(m) = \frac{\sigma^2}{K f_s} \text{sinc}\left(\frac{mM}{K} - \frac{\lambda - \ell}{K}\right). \quad (20)$$

To determine $R_{D_k X_k}(m)$, this impulse response must be scaled by a factor f_s so that its DFT produces a discrete power spectrum whose bins sum to the correct power. With this scaling, the cross-correlation becomes

$$R_{D_k X_k}(m) = \frac{\sigma^2}{K} \text{sinc}\left(\frac{mM}{K} - \frac{\lambda - \ell}{K}\right). \quad (21)$$

The autocorrelation functions $R_{X_k X_k}(m)$ and $R_{D_k D_k}(m)$ can similarly be shown to equal

$$R_{X_k X_k}(m) = R_{D_k D_k}(m) = \frac{\sigma^2}{K} \text{sinc}\left(\frac{mM}{K}\right). \quad (22)$$

Using equation (19), the SNR is the same within each bin and is equal to

$$\text{SNR}_k = \frac{1}{1 - \text{sinc}^2((\lambda - \ell)/K)}. \quad (23)$$

This is also equal to the total frequency domain SNR, since the channels through which both observation and desired response signals have passed have frequency-independent magnitude and delay response. Under the assumption of independent bins, this SNR is also equal to the SNR of the reconstructed time domain output. Equation (23) illustrates an important result; due to the SNR dependence on the magnitude of the differential delay $|\lambda - \ell|$, the filterbank FDAF effects signal *advance* to the same accuracy as it can effect delay. Consequently for frequency domain equalisation, in the absence of detailed channel knowledge, the most generally optimum design would use $\lambda = 0$.

The SNR given by (23) is plotted as the solid trace in Figure 6, for the case where $M = K/2$, $\ell = 64$, $\lambda = 0$, and K is varied over the range ℓ to 32ℓ . The horizontal axis is the ratio K/ℓ , to clarify that the curve depends only on this ratio and not on the values of ℓ and K themselves. Experimental results were also obtained by approximating the independence of the bins by using a DFT filterbank with very little overlap of adjacent frequency bins. This was achieved by using analysis filters with very long impulse responses, $N_h = RK$, where $R = 32$. The details of this filter design, based on a Hamming window, are given in [6].

The experimental frequency domain SNR, that is, the ratio of total frequency domain signal power to total frequency domain error power, is plotted as circles. The crosses represent the experimental SNR of the time domain output. The results illustrate that a DFT filterbank with independent bins cannot exactly compensate even a constant delay channel except asymptotically as $K \rightarrow \infty$. The closeness of the theoretical and experimental results also verifies that the SNR of the time domain filterbank output is approximately equal to the SNR within the filterbank transform domain, for the case where bin independence can be closely modelled.

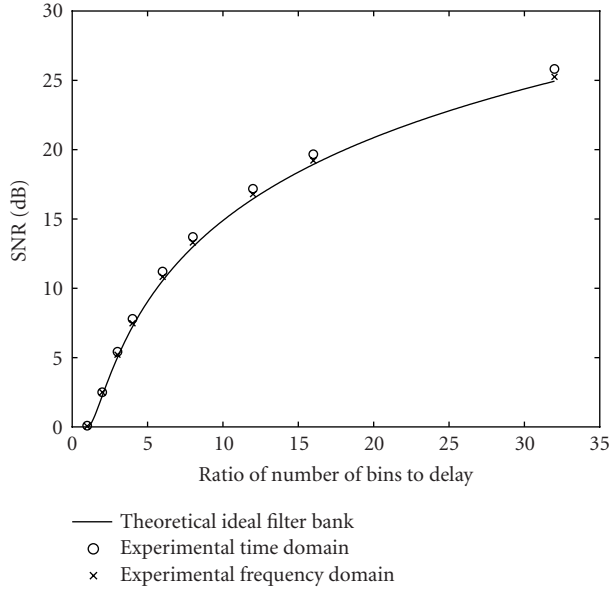


FIGURE 6: Reconstruction SNR for “ideal” filterbank FDAF equalisation of constant delay.

4.1.2. Channel with linear delay

Now consider an allpass channel, $c'(n)$, with a delay that varies linearly from ℓ_{\min} to ℓ_{\max} samples over the sampling bandwidth. Let the delay associated with channel $c'_k(n)$ vary from ℓ_{\min} to ℓ_{\max} samples over the bandwidth of the k th bin, at the input sampling rate. The delay difference between the desired response and observation signal thus varies over $\lambda - \ell_{\max}$ to $\lambda - \ell_{\min}$ samples. It is easy to show [6] that

$$\begin{aligned}\ell_{\min}(k) &= \ell_{\min} + \frac{\ell_{\max} - \ell_{\min}}{K} \left(k + \frac{K+1}{2} \right), \\ \ell_{\max}(k) &= \ell_{\min} + \frac{\ell_{\max} - \ell_{\min}}{K} \left(k + \frac{K-1}{2} \right).\end{aligned}\quad (24)$$

The cross-spectral delay between the decimated desired response and observation signals then varies linearly from $\ell_1 = (\lambda - \ell_{\max})/M$ to $\ell_2 = (\lambda - \ell_{\min})/M$ samples at the decimated rate, $f'_s = f_s/M$ Hz.

Let ν represent the discrete frequency index for a frequency domain representation of the k th subband data. To determine the cross-correlation function $R_{D_k X_k}(m)$, the cross-spectrum $S_{D_k X_k}(\nu)$ can be sampled at N points and an inverse DFT computed. Under our assumption that $s(t)$ is white, the power spectral magnitude $|S_{ss}(f)|$ is constant and equal to σ^2/f_s units squared per Hz. Thus the magnitude of the cross-spectral density $\mathcal{S}_{D_k X_k}(\nu)$ is equal to $\sigma^2 |H(\nu)|^2 / NM$ units squared per bin² and the cross-spectral density $\mathcal{S}_{D_k X_k}(\nu)$ is equal to

$$\mathcal{S}_{D_k X_k}(\nu) = |\mathcal{S}_{SS}(\nu)| |H(\nu)|^2 e^{j\Phi_k(\nu)}. \quad (25)$$

²Since the subband data is sampled at $f'_s = f_s/M$ Hz, the bandwidth of each of the N bins is equal to f_s/NM Hz and the power within each bin is equal to σ^2/NM units squared.

Within the k th filterbank channel, the N point correlation function between the decimated reference and the primary signal component, $R_{D_k X_k}(m)$, is then approximately given by³

$$\begin{aligned}R_{D_k X_k}(m) &= N \times \text{IDFT}[\mathcal{S}_{D_k X_k}(\nu)] \\ &= \frac{\sigma^2}{M} \text{IDFT} \left[|H(\nu)|^2 e^{j\Phi_k(\nu)} \right],\end{aligned}\quad (26)$$

with

$$\Phi_k(\nu) = (\ell_2 - \ell_1) \frac{\pi \nu^2}{2bN} + (\ell_1 + \ell_2) \frac{\pi \nu}{N}, \quad (27)$$

where the bandwidth $2b = MN/K$. Although not explicitly indicated in (27), the delays ℓ_1 and ℓ_2 are a function of the bin number, k . The autocorrelation functions $R_{X_k X_k}(m)$ and $R_{D_k D_k}(m)$ can similarly be computed by specifying a linear phase term in (26). The SNR within each bin is computed using (19) but the total filterbank SNR should be computed by the ratio of total signal to total error power. That is,

$$\text{SNR}_{\text{FB}} = \frac{\sum_{k=0}^{K-1} R_{D_k D_k}(0)}{\sum_{k=0}^{K-1} J_k}, \quad (28)$$

where the power of the desired response signal is equal to $R_{D_k D_k}(0)$, and from (5), the error power within the k th bin is

$$J_k = R_{D_k D_k}(0) - \frac{|R_{D_k X_k}(0)|^2}{R_{X_k X_k}(0)}. \quad (29)$$

If the filterbank exhibits perfect reconstruction and the bins are independent, the SNR associated with the reconstructed time domain output satisfies the relationship $\text{SNR}_{\text{td}} = \text{SNR}_{\text{FB}}$, otherwise this relationship is only approximate.

We used this general analysis to determine the equalisation performance for a constant delay channel using a practical filterbank FDAF. The analysis and synthesis filters were designed to have identical impulse responses, where only adjacent bins exhibit any significant spectral overlap, resulting in near-perfect reconstruction⁴ and so that the sum of the power within each analyser bin equals the time domain input signal power. The length of the analysis and synthesis filters was $N_h = RK$, where $R = 4$, and the filterbank had a decimation factor $M = K/2$. Equation (26) was computed using these parameters, with $K = 512$ and $N = 100$. The magnitude response of the analysis filter was determined by performing an N -point DFT on the decimated impulse response $h(mM) = h(n)$.

³In general, the discrete power spectrum $\mathcal{S}_{xx}(\nu)$ of a signal $x(m)$ can be estimated by $1/N$ times the periodogram $|X(\nu)|^2$, where $X(\nu) = \text{DFT}[x(m)]$. Since the autocorrelation function, $R_{xx}(m)$, estimated by time average $x(m) * x^*(-m)$ is equal to the inverse DFT of $|X(\nu)|^2$, it follows that $R_{xx}(m)$ is equal to N times the inverse DFT of $\mathcal{S}_{xx}(\nu)$.

⁴That is, less than -65 dB reconstruction error was achieved for a back-to-back analyser/synthesiser configuration.

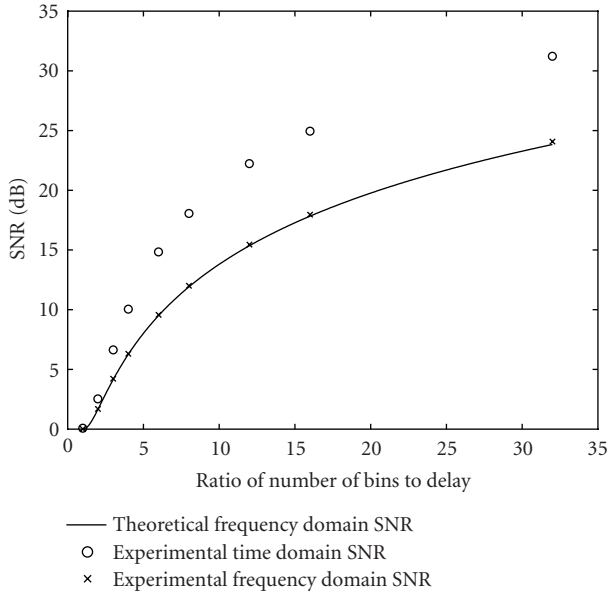


FIGURE 7: Reconstruction SNR for filterbank FDAF equalisation of constant delay.

The solid trace of Figure 7 shows the theoretical frequency domain SNR as a function of the ratio K/ℓ . Frequency domain SNR measurements, computed from experimental results, are shown as crosses and the corresponding time domain output SNR points are shown as circles. By comparison with Figure 6, it can be seen that the frequency domain SNR is almost the same as that obtained when the bins are independent. However, the experimental results show that the SNR of the filterbank time domain output is better. This can be explained by considering the power spectra of the subband error signals. Simulations have shown that the error power spectrum is distributed towards the edges of the bins, rather than about the bin centre as is the signal power spectrum. By design, the action of the synthesis filters is to constructively combine the signal components of adjacent bins, but the error is attenuated by these filters. So while the signal power is preserved by the synthesis process, the error power is reduced. The result is the superior SNR of the time domain filterbank output compared with the transform SNR.

Next, we look at the performance of a filterbank FDAF for equalising the linear delay channel which was defined in Example 2. The channel has delay that varies linearly from $\ell_{\max} - \ell_{\min} = 100$ input samples over the full discrete frequency range. The theoretical frequency domain SNR is shown as the solid trace in Figure 8, for a perfect reconstruction filterbank with nonoverlapping bins. The delay in the desired response channel was chosen to maximise the SNR. Since the filterbank is capable of effecting a noncausal response, where a delay of $-\ell$ samples is as readily approximated as a delay of ℓ samples, the optimum choice is $\lambda = n_0 = (\ell_{\max} + \ell_{\min})/2$. The example channel has ℓ_{\min} and ℓ_{\max}

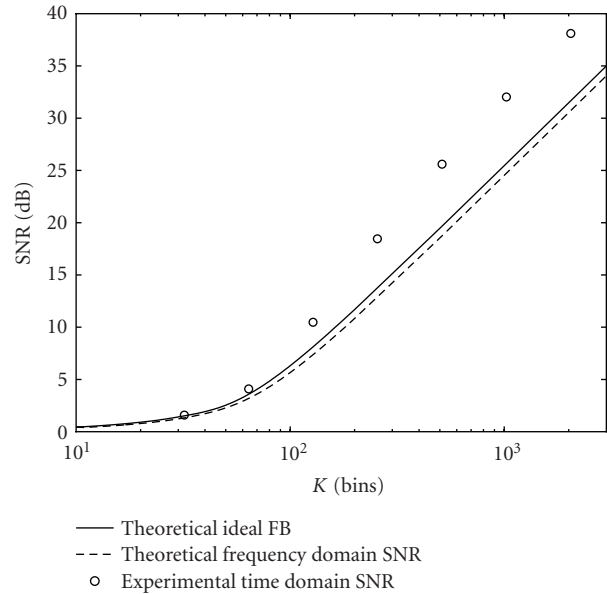


FIGURE 8: Reconstruction SNR for filterbank FDAF equalisation of the linear delay channel.

equal to 975 and 1075, respectively, so that the channel delay is symmetric about $n_0 = 1025$. Justified by the closeness of the time and frequency domain SNR measures for the constant delay channel (Figure 6), we assert that this solid trace also represents the time domain SNR measure for the “ideal” filterbank. Also shown in Figure 8 is the theoretical frequency domain (dashed) and experimental time domain (circles) SNR achieved by the $R = 4$ practical filterbank FDAF that was introduced earlier in this section. As anticipated from the results of the constant delay channel, the frequency domain SNR associated with the practical filterbank is very similar, but slightly inferior, to the ideal filterbank. However, also in similarity to the results of the constant delay channel, the time domain SNR is superior to the frequency domain measure.

We can use Figures 8 and 4 to compare the performance of the frequency domain filter with a time domain FIR filter for the equalisation of the linear delay channel. Since the relationships between SNR and the parameters of each filter type are nonlinear, the comparison is most easily accomplished by looking at the number of filter weights that are required to achieve specific SNR levels. Inspection of Figure 4 reveals that to achieve SNR equal to 18 dB and 35 dB, respectively, approximately $L = 100$ and $L = 200$ taps are required by a FIR filter. From Figure 8, it can be seen that to achieve similar frequency domain SNR, the number of ideal filterbank bins must be around $K = 450$ and $K = 3000$ bins, respectively. This is 4.5 and 15 times greater than the corresponding number of FIR filter taps. The practical $R = 4$ filterbank requires approximately $K = 250$ and $K = 1500$ bins which, for this example, is around half the number of bins required by the ideal filterbank.

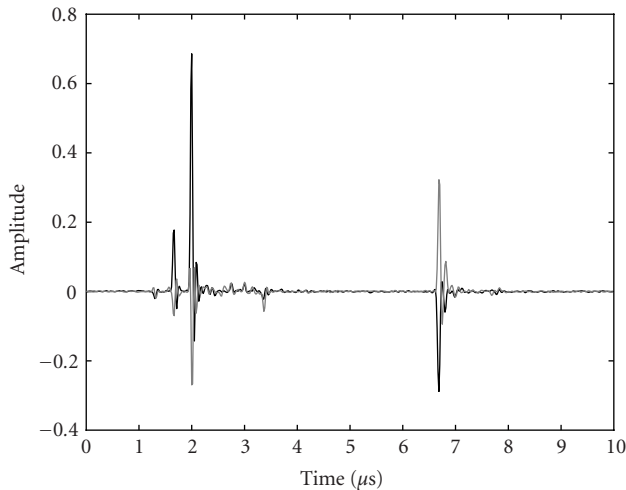


FIGURE 9: Real (black) and imaginary (grey) parts of example channel impulse response.

The results of the previous paragraph can be compared with the relationship in (3). In this example, the ideal filterbank has an infinite number of analysis filter samples. According to (3), the number of subband FIR taps must also be infinite, yet we have shown that there exists a filterbank FDAF (equivalent to an SAF with one tap per subband FIR filter) that can achieve the FIR performance. This clearly illustrates the conservative nature of (3).

4.2. Channel equalisation example

It is important to compare the specialised results discussed thus far with the equalisation performance of a real-world channel and signal. In this section, we provide an example where a simulation signal is passed through such a channel and is subsequently equalised using both an FDAF and a time domain LMS equaliser.

Consider the microwave channel with an equivalent baseband impulse shown in Figure 9, obtained with a 60 MHz sampling rate. This is “channel 14,” taken from the Rice University microwave channel database, currently available at the Internet site “<http://spib.rice.edu/spib/microwave.html>.” Analysis shows that there is considerable variation in both the delay and the magnitude of the frequency response, with nonminimum phase zeros located close to the unit circle. We used, for the example signal, a baseband 12 Mbaud BPSK signal with root raised cosine pulse shaping.

Each of the FDAF and LMS filter parameters was adjusted so that in the steady state, the output signal was restored to a similar SNR. So that the example represents, as realistically as possible, a typical equalisation problem, the delay parameter λ was chosen without incorporating knowledge of the length of the channel impulse response. Consequently, in accordance with the discussions in Sections 3 and 4.1, λ was chosen equal to $L/2$ for the time domain filter and 0 for the FDAF. With $L = 4096$ taps and convergence coefficient $\mu = 10^{-5}$, the FIR filter achieved approximately 19 dB steady state SNR. In the filterbank case, we used an oversampling

factor $I = 2$ and length $4K$ analysis and synthesis filters. The FDAF filter weights were determined using the single tap RLS algorithm with $\gamma = 0.99$ and it was found that with $K = 4096$ bins, the filterbank FDAF also achieved approximately 19 dB SNR.

In this example, to achieve the same output SNR, a similar number of degrees of filtering freedom are required for each of the time domain FIR filter and the FDAF. This observation has also been found to be consistent with other real-world channel examples, including a number of others from the Rice University database. For these other cases, the FDAF required at most twice the number of degrees of freedom of the time domain filter.

This is a significantly different observation to that which could be anticipated from studying the results of the linear delay channel. In that case, the experimental results showed that to achieve approximately 26 dB SNR, the FIR and FDAF required $L = 250$ taps and $K = 1000$ bins, respectively; considerably more degrees of freedom are required by the FDAF. That in these real-world examples a comparable number of degrees of freedom are required by each of the two filter types can be well explained by considering the duality between FIR and FDAF filters. The FIR filter is inherently well suited to effecting pure delay functions; it can localise in time, since it is a time domain operation. On the other hand, an FDAF can effect narrowband modification of the frequency response. It is not surprising then that for an operation such as real-world channel equalisation, that requires modification of both delay and frequency response, a similar number of degrees of freedom are required by both FIR and FDAF filters. We should again emphasise that there are additional reasons why, in practice, the FDAF may or may not be adopted in preference to a time domain approach, as discussed in the introduction to this paper. The most notable advantages in these real-world examples are the superior convergence rate and computational efficiency of the FDAF.

This relationship between the number of degrees of freedom required by an FDAF and an FIR filter to achieve similar delay compensation clearly depends on the particular channel type. Importantly, however, in any of the cases considered here⁵, it has been shown that it is possible to design an FDAF to achieve equivalent delay compensation performance to that of an FIR filter.

5. CONCLUSION

In this paper, we have addressed an important issue associated with the application of a DFT filterbank FDAF to channel equalisation. We have shown that a fundamental difference between the DFT filterbank and an FIR filter is the accuracy of delay compensation. While an L -tap FIR filter is capable of perfect compensation for a set of L discrete delays, a DFT filterbank FDAF, with independent bins, is incapable

⁵This excludes the case where the delay is constant and equal to a multiple of the sampling period, in which case it is possible to achieve perfect compensation using an FIR filter.

of perfect delay compensation except asymptotically as the number of bins approaches infinity. For other delays, however, we have shown that it is possible to determine filterbank FDAF parameters that result in equivalent performance to that of an FIR filter.

For equalisation of a linear delay channel, a filterbank FDAF can require in excess of an order of magnitude more bins than the number of taps required by a FIR filter. The ability of a filterbank FDAF to compensate delay is directly related to the degree of spectral overlap that exists between bins and results indicate that the greater the independence between bins, the poorer the quality of FDAF delay compensation.

Notwithstanding these conclusions, the linear delay channel represents an extreme condition and counter examples have suggested that for compensation of more typical communications channels, the number of bins required by an FDAF is around the same as the number of taps required by a similarly performing FIR filter.

It has been shown that for the majority of the channels considered, it is possible to design a filterbank FDAF to achieve a delay compensation performance that is equivalent to that possible using an FIR filter. This is a new observation that would otherwise not be clear from previously published work.

APPENDIX

In this appendix, the expression for the cross-spectrum, $\mathcal{S}_{d_k x_k}(f) = |H(f)|^2 \mathcal{S}_{ss}(f - f_k)$, used in Section 4.1, is derived.

First, recall that $x(n) = s(n) * c'(n)$ and $d(n) = s(n) * g'(n)$. Then, with reference to Figure 5,

$$x_k(n) = [(s(n) * c'(n))e^{-j2\pi f_k n / f_s}] * h(n), \quad (\text{A.1})$$

which commutes to

$$x_k(n) = (s(n) * c'(n) * h'(n))e^{-j2\pi f_k n / f_s}, \quad (\text{A.2})$$

where $h'(n) = h(n)e^{j2\pi f_k n / f_s}$. Similarly,

$$d_k(n) = (s(n) * g'(n) * h'(n))e^{-j2\pi f_k n / f_s}. \quad (\text{A.3})$$

Then, from linear systems theory, the cross-spectrum $\mathcal{S}_{x_k d_k}(f)$ is given by

$$\begin{aligned} \mathcal{S}_{x_k d_k}(f) &= \mathcal{S}_{ss}(f - f_k) C'(f - f_k) H'(f - f_k) \\ &\quad \times [G'(f - f_k) H'(f - f_k)]^* \\ &= \mathcal{S}_{ss}(f - f_k) C'(f - f_k) G'^*(f - f_k) \\ &\quad \times |H'(f - f_k)|^2, \end{aligned} \quad (\text{A.4})$$

where $C'(f)$, $G'(f)$, and $H'(f)$ are the Fourier transforms of $c'(n)$, $g'(n)$, and $h'(n)$, respectively. However, by definition,

$H'(f - f_k) = H(f)$, and under the assumption that $c'(n)$ and $g'(n)$ have unity gain, flat frequency responses over the bandwidth of the k th analysis filterbank bin, we have, as required, that

$$\mathcal{S}_{x_k d_k}(f) = \mathcal{S}_{ss}(f - f_k) |H(f)|^2. \quad (\text{A.5})$$

ACKNOWLEDGMENTS

The author thanks Ken Lever, John Tsimbinos, and Lang White for their helpful discussions relating to this work. The work was undertaken while the author was also affiliated with the Institute for Telecommunications Research, University of South Australia.

REFERENCES

- [1] E. R. Ferrara Jr., "Frequency-domain adaptive filtering," in *Adaptive Filters*, C. F. N. Cowan and P. M. Grant, Eds., Prentice-Hall, Englewood Cliffs, NJ, USA, 1985.
- [2] R. E. Crochiere and L. R. Rabiner, *Multirate Digital Signal Processing*, Prentice-Hall, Englewood Cliffs, NJ, USA, 1983.
- [3] J. R. Treichler, S. L. Wood, and M. G. Larimore, "Some dynamic properties of transmux-based adaptive filters," in *Proc. 23rd Asilomar Conference on Signals, Systems and Computers*, vol. 2, pp. 682–686, Pacific Grove, Calif, USA, October–November 1989.
- [4] L. B. Milstein and P. K. Das, "Spread spectrum receiver using surface acoustic wave technology," *IEEE Trans. Communications*, vol. COM-25, no. 8, pp. 841–847, 1977.
- [5] L. B. Milstein and P. K. Das, "An analysis of a real-time transform domain filtering digital communication system: part I: narrow-band interference rejection," *IEEE Trans. Communications*, vol. COM-28, no. 6, pp. 816–824, 1980.
- [6] G. Parker, *Frequency domain restoration of communications signals*, Ph.D. dissertation, University of South Australia, Adelaide, South Australia, Australia, March 2001.
- [7] B. Widrow and S. D. Stearns, *Adaptive Signal Processing*, Prentice-Hall, Englewood Cliffs, NJ, USA, 1985.
- [8] F. A. Reed and P. L. Feintuch, "A comparison of LMS adaptive cancellers implemented in the frequency domain and the time domain," *IEEE Trans. Circuits and Systems*, vol. 28, no. 6, pp. 610–615, 1981.
- [9] M. Dentino, J. McCool, and B. Widrow, "Adaptive filtering in the frequency domain," *Proceedings of the IEEE*, vol. 66, no. 12, pp. 1658–1659, 1978.
- [10] S. Weiss, *On Adaptive Filtering in Oversampled Subbands*, Ph.D. dissertation, University of Strathclyde, Glasgow, UK, 1998.
- [11] S. Weiss, S. R. Dooley, R. W. Stewart, and A. K. Nandi, "Adaptive equalisation in oversampled subbands," *IEE Electronics Letters*, vol. 34, no. 15, pp. 1452–1453, 1998.
- [12] A. Gilloire and M. Vetterli, "Adaptive filtering in subbands with critical sampling analysis, experiments, and application to acoustic echo cancellation," *IEEE Trans. Signal Processing*, vol. 40, no. 8, pp. 1862–1875, 1992.
- [13] A. Fertner, "Frequency-domain echo canceller with phase adjustment," *IEEE Trans. on Circuits and Systems II: Analog and Digital Signal Processing*, vol. 44, no. 10, pp. 835–841, 1997.
- [14] W. Kellermann, "Analysis and design of multirate systems for cancellation of acoustical echoes," in *Proc. IEEE Int. Conf. Acoustics, Speech, Signal Processing*, vol. 5, pp. 2570–2573, New York, NY, USA, April 1988.

- [15] T. Gansler, "A robust frequency-domain echo canceller," in *Proc. IEEE Int. Conf. Acoustics, Speech, Signal Processing*, vol. 3, pp. 2317–2320, Munich, Germany, April 1997.
- [16] R. W. Stewart, S. Weiss, D. Garcia-Alis, and G. Freeland, "Sub-band adaptive equalization of time-varying channels," in *Proc. 33rd Asilomar Conference on Signals, Systems and Computers*, vol. 1, pp. 534–538, Pacific Grove, Calif, USA, October 1999.
- [17] T. I. Laakso, V. Valimaki, M. Karjalainen, and U. K. Laine, "Splitting the unit delay," *IEEE Signal Processing Magazine*, vol. 13, no. 1, pp. 30–60, 1996.
-

Gareth Parker obtained an Honours degree in electrical and electronic engineering from the University of Adelaide in 1990. In 2001, he was awarded a Ph.D. by the University of South Australia, for his thesis entitled "Frequency domain restoration of communications signals." He works for the Defence Science and Technology Organisation, Australia, with current interests in spread spectrum communications, adaptive filters, and frequency domain processing.

